論文 / 著書情報
Article / Book Information

Title	Preparation and Characterization of Polyimide/ZnO Nano-hybrid Films Exhibiting High Refractive Indices
Authors	Atsuhisa SUZUKI, Shinji ANDO
Citation	Journal of Photopolymer Science and Technology, Vol. 23, No. 4, pp. 521-528
Pub. date	2010, 6

Journal of Photopolymer Science and Technology
Volume 23, Number 4 (2010) 521-528 ©2010CPST

Preparation and Characterization of Polyimide/ZnO Nano-hybrid Films Exhibiting High Refractive Indices

Atsuhisa SUZUKI and Shinji ANDO

Department of Chemistry and Materials Science, Tokyo Institute of Technology, 2-12-1 O-okayama, Meguro-ku, Tokyo 152-8552, Japan

A series of polyimides (PIs) / zincoxide (ZnO) nano-hybrid materials exhibiting high transparency, high refractive indices, and low wavelength dispersions were prepared by the *in situ* thermal decomposition method. First, the optical properties of six kinds of matrix PIs were investigated, and a fully aromatic PI derived from 4,4'-(hexafluoroisopropylidene) diphthalic dianhydride (6FDA) and 9,9-bis (4-aminophenyl) fluorene (BAFL) and a semi-aromatic PI derived from 3,3';4,4'-biphenyl tetracarboxylic dianhydride (BPDA) and 4,4'-diaminodicyclohexylmethane (DCHM) were chosen as transparent matrices. Secondly, two types of ZnO precursors, which are thermally decomposed into ZnO, were chosen, and the thermal decomposition behaviors of the ZnO precursors dissolved in PI films was examined by far-infrared (Far-IR) and variable temperature mid-infrared (IR) spectra. The PI/ZnO hybrid films prepared from $Zn(NO_3)_2 \cdot 6H_2O$ as a ZnO precursor exhibit yellowish coloration, though the transparency of the hybrid films was significantly improved by using a preheated $Zn(NO_3)_2 \cdot 6H_2O$ at 110 ºC as a ZnO precursor or using a soluble PI solutions in place of poly(amic acid) solutions. The PI/ZnO hybrid films exhibited high thermal degradation temperatures, and 6FDA-BAFL and BPDA-DCHM/ZnO hybrid films exhibited higher refractive indices by up to +0.0037 (+0.25 %) and +0.0130 (+1.10 %), respectively, compared with the pristine PIs. In the case of BPDA-DCHM, the effect of hybridization with ZnO on the increase in the refractive index at infinite wavelength (n_∞) relative to the coefficient of wavelength dispersion (D) is more significant than that of modifying the chemical structures of PIs.

Key words: polyimide, ZnO, nano-hybrid, refractive index, transparency

1. Introduction

There have been strong demands for highly refractive polymers with high optical transparency, good thermal stability, and low wavelength dispersion for designing microlens components for charge-coupled devices (CCD) or complementary metal oxide semiconductor (CMOS) image sensors (CIS) [1]. Polyimides (PIs) have been widely used in microelectronic applications because of their high thermal stabilities and mechanical properties [2]. PIs are also expected to be used as optical materials in opto-electronics and photonic applications. However, conventional PIs do not exhibit sufficient optical transparencies, which is due to the formation of charge-transfer (CT) complexes between the electron-donating diamine and the electron-accepting dianhydride moieties. Introductions of low polarizable fluorine atoms, sterically bulky structures, and allicyclic moieties into the PI chains have been reported to be effective to overcome this problem [3,4].

For the improvement of the optical properties of PIs, organic/inorganic hybrid materials have been extensively studied because they offer possibilities to combine the advantageous properties of PIs and inorganic materials such as TiO_2, ZrO_2, ZnO and SiO_2 [5-8]. In particular, ZnO possesses a wide direct band gap of 3.4 eV, high transparency in the visible region, a high refractive index of 1.93, and characteristic luminescent properties. Because of these features, ZnO is an attractive material for wide range of applications such as antireflection coatings, transparent electrodes in solar sells, and light emitting diodes [9-11]. It has been reported

Received April 7, 2010
Accepted May 14, 2010

that the combination of ZnO nano-particles with polymers enhances the fluorescent properties via energy transfer at the excited state [12,13].

However, the compatibility of polymers with inorganic materials is generally insufficient because inorganic nano-sized particles easily form aggregates due to the high surface energy. Particle aggregates incorporated in polymer films readily cause serious light scatterings, which deteriorates the transparency of films. To improve the compatibility between polymers and nano-particles, organic/inorganic hybrid materials have been prepared by the 'surface modification' methods using coupling agents or the 'sol-gel' method using metal alkoxides [14,15]. However, thermal stability of hybrid films are generally deteriorated by addition of coupling agents or by the incomplete hydrolysis of metal alkoxides [16,17].

In this study, novel PI/ZnO nano-hybrid films were prepared by '*in situ* thermal decomposition method' without reducing their inherent advantages [18]. Firstly, the optical properties of PI films were investigated to choose preferential matrix PIs with high refractive index and transparency. Secondly, the thermal decomposition behaviors of ZnO precursors were examined. And thirdly, PI/ZnO nano-hybrid films were prepared by thermal curing of precursor solutions containing a ZnO precursor. The precursors were thermally decomposed into ZnO in the films via curing at 300 or 350 ºC. The decomposition reactions of the precursors and the optical properties of the hybrid films thus obtained were extensively investigated .

2. Experimental

2.1. Materials

3,3';4,4'-Biphenyltetracarboxylic dianhydride (BPDA) purchased from Wako Pure Chemicals Industries, Ltd., 3,3';4,4'-Diphenylethertetra carboxylic dianhydride (ODPA) and 4,4'-(Hexa fluoroisopropylidene)diphthalic dianhydride (6FDA) supplied by MANAC Inc., and 9,9-Bis(4-aminophenyl)fluorene (BAFL) supplied by Wakayama Seika Corp. were purified by sublimation under reduced pressure. 4,4'-Diamino-dicyclohexylmethane (DCHM) purchased from Tokyo Kasei Kogyo Co., Ltd. was recrystallized from *n*-hexane solution and sublimed under reduced pressure. *N*,*O*-Bis(trimethylsilyl)trifluoroacetamide (BSTFA) and *N*,*N*-Dimethyl acetamide (DMAc), both were purchased from Aldrich, were used as received. $Zn(NO_3)_2{\cdot}6H_2O$ purchased from Wako was used as received without further purification.

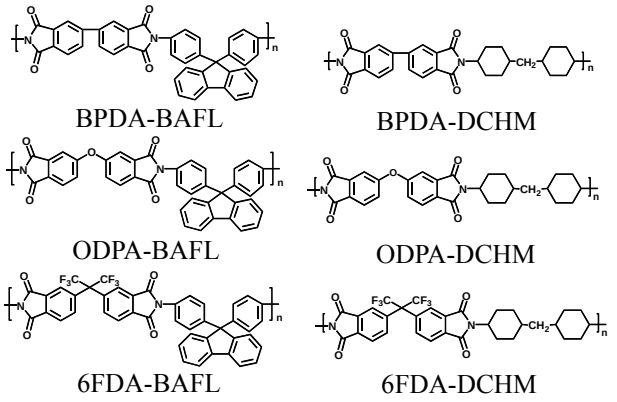

Fig. 1 Structures of PIs.

Table 1 Preparation of precursor solutions.

	Polymer solution	ZnO precursor
Method-1	PAA or PASE	Pre-Zn [a]
Method-2	PAA or PASE	Pre-Zn (110ºC) [b]
Method-3	PI	Pre-Zn (110ºC) [b]

[a] $Zn(NO_3)_2{\cdot}6H_2O$

[b] $Zn(NO_3)_2{\cdot}6H_2O$ heated at 110 ºC for 5 h under nitrogen

2.2. Preparation of PI films

The molecular structures of six kinds of PIs examined in this study are shown in Fig. 1. The precursors of fully aromatic PIs, poly(amic acid)s (PAAs), were prepared by adding equimolar amounts of dianhydride to a DMAc solution of diamine. The PAA solutions were stirred with an ice bath for 2 h followed by stirring at ambient temp. for 24 h. The precursors of semi-aromatic PIs, poly(amic acid) silyl ester (PASE), were prepared by the *in situ* silylation method as reported by Oishi et al. [19]. First, DCHM was dissolved in DMAc, and 1.05 molar amount of BSTFA were added to the solution to form *N*-silylated alicyclic diamine. This silylation can avoid the salt formation between unreacted amino ($-NH_2$) and carboxyl (-COOH) groups at amic acid moiety. Then, equimolar amount of dianhydride was added to the solution. The generated PASE solutions were stirred in the same way as the PAA solutions.

Table 1 lists the three kinds of methods adopted for preparing the precursor solutions of hybrid films. In this study, two kinds of ZnO precursors were used. One was $Zn(NO_3)_2{\cdot}6H_2O$ as received (denoted as 'Pre-Zn'), and the other was prepared by heating Pre-Zn at 110 ºC for 5 h under nitrogen (denoted as 'Pre-Zn(110ºC)'). The precursor solutions were prepared by 1) dissolving Pre-Zn in PAA or PASE solutions (Method-1), 2) dissolving Pre-Zn(110ºC) in PAA or PASE solutions (Method-2) or 3) dissolving Pre-Zn(110ºC) in

soluble PI solutions (Method-3). The concentration of ZnO component in the PI/ZnO hybrid films was expressed as a molar percentage of ZnO to the repeating unit of PIs. Pristine PI and PI/ZnO hybrid films were prepared via spin-coating of precursor solutions onto Si substrates, followed by drying at 70 ºC for 1h and thermal imidization at 300 ºC and 350 ºC for 1.5h under a nitrogen atmosphere for the semi- aromatic and the fully aromatic PIs, respectively.

2.3. Measurements

Refractive indices of the PI and hybrid films whose thicknesses were controlled between 10-15 μm were measured using a prism coupler (Metricon, model PC-2010) at the wavelengths of 633, 845, 1324 and 1558 nm for the in-plane (n_{TE}) and out-of-plane (n_{TM}) polarizations. The average refractive indices were calculated according to equation 1,

$$n_{av} = \sqrt{(2n_{TE}^2 + n_{TM}^2)/3} \quad (1)$$

Fourier transform infrared absorption (FT-IR) spectra were obtained with a Thermo-Nicolet AVATAR-320 FT-IR spectrometer. Fourier transform Far-infrared absorption (Far-IR) spectra were measured with a JASCO FT-IR/6100 spectrometer. UV-vis absorption spectra were acquired with a Hitachi U-3500 spectrometer. Thermolytic behaviors were measured with a Shimadzu DTG-60 analyzer under nitrogen. Densities of PI films were measured with a pycnometer by using water as a medium.

3. Results and Discussion

3.1. Optical properties of pristine PIs

Fig. 2 shows the wavelength dispersions of n_{av} for the six kinds of pristine PIs. The n_{av} values are varied depending on the dianhydride structures in the order of BPDA > ODPA > 6FDA. The higher refractive indices of the PIs from BPDA are explainable by the dense molecular packing of the PI chains because BPDA has a rigid and planar molecular structure. On the other hand, the lower n_{av} of the PIs derived from 6FDA are explainable by the loose molecular packing and the less polarizable $-CF_3$ side groups in the PI chains. The n_{av} values measured at the four wavelengths (n_λ) were fitted using the simplified Cauchy's formula [20],

$$n_\lambda = n_\infty + D/\lambda^2 , \quad (2)$$

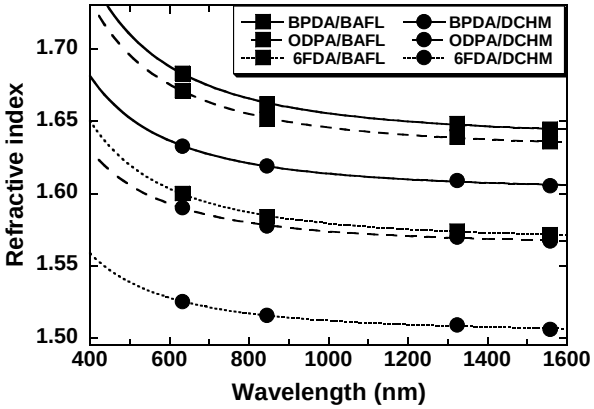

Fig. 2 Wavelength dispersions of the PIs.

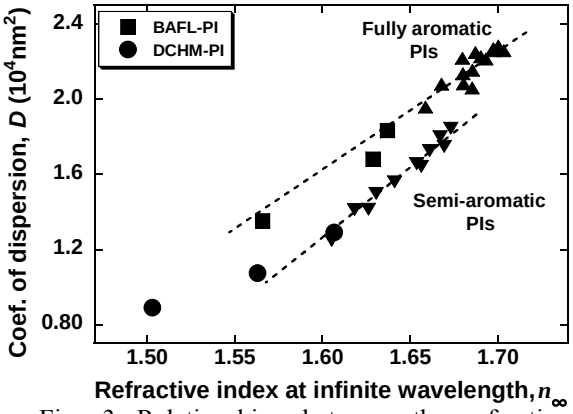

Fig. 3 Relationships between the refractive induces at infinite wavelength (n_∞) and the coefficients of dispersion (D) for the PIs.

where n_∞ is the estimated virtual refractive index at the infinite wavelength, and D is the coefficient of wavelength dispersion. A higher D corresponds to a larger wavelength dispersion of n_{av}. Fig. 3 illustrates the relationships between n_∞ and D values for the pristine PIs. The plots of the six PIs agree well with the linear relationships of fully aromatic and semi-aromatic PIs, respectively, which were reported by the present authors [20,21]. The PIs derived from BAFL exhibited smaller D values than those expected from the relationships because the significant steric hindrance around the diphenylfluorene moiety in BAFL should cause loose molecular packing in the PI chains.

The UV-vis spectra of the PI films are shown in Fig. 4. The semi-aromatic PIs derived from DCHM exhibited higher transparency than the fully aromatic PIs. In general, the coloration of fully aromatic PIs originates from the formation of intra- and inter-molecular CT complexes, which absorb UV and visible light. The absorption edges of the PIs are varied depending on the dianhydride structures in the same order as the refractive indices in Fig. 2 (BPDA > ODPA > 6FDA). The lower transparency of the PIs derived from BPDA are attributable to the dense molecular packing of

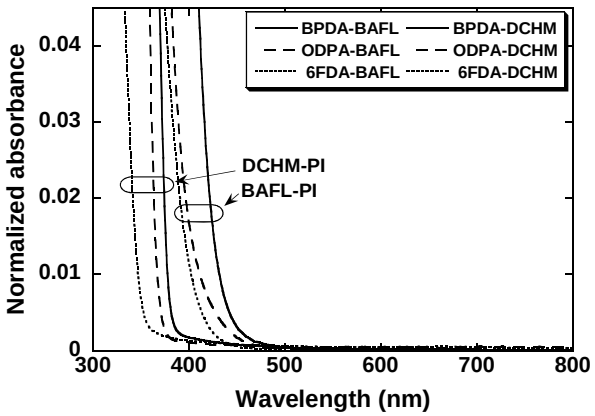

Fig. 4 UV-vis spectra of the PI films.

PI chains with CT interactions, and the higher transparency of the PIs derived from 6FDA is owing to the steric hindrance of -CF_3 groups which weaken the CT interactions among PI chains.

As shown in Figs.2 and 4, the fully aromatic PIs exhibited higher refractive indices than the semi-aromatic PIs, whereas the latter PIs exhibited higher transparency than the former PIs. These results indicate that 6FDA-BAFL with the highest transparency in the fully aromatic PIs and BPDA-DCHM with the highest refractive index in the semi-aromatic PIs could be the best PIs as the matrices for preparing PI/ZnO hybrids which simultaneously exhibit high refractive indices and transparency. It should be noted that the films of 6FDA-BAFL are soluble in DMAc due to the steric -CF_3 and fluorene groups, while the films of BPDA-DCHM are insoluble in any solvents except for sulfuric acid. Due to this insolubility, Method-3 could not be applied to the preparation of BPDA-DCHM/ZnO hybrid films (see Table 1).

3.2. Thermal decomposition reaction of Pre-Zn

The thermal decomposition of Pre-Zn can be considered to proceed as follows [22],

$$Zn(NO_3)_2{\cdot}6H_2O \rightarrow ZnO + 2HNO_3 + 5H_2O. \quad (3)$$

As seen in Fig. 5, the thermal decomposition of Pre-Zn to ZnO was completed under nitrogen at 250 ºC, and the residual weight of 27.7 % was very close to the calculated value of ZnO (27.4 %) based on the molecular weights of Pre-Zn and ZnO. This clearly supports the reaction (3) at elevated temperatures. Furthermore, Fig. 6 shows the TGA curves of Pre-Zn kept at each of 110 and 120 ºC under nitrogen. The residual weights approached to 65.2 and 44.1%, respectively. Since the residual weights calculated for $Zn(NO_3)(OH){\cdot}3H_2O$ (66.7 %) and $Zn_3(NO_3)_2(OH)_4$ (43.5%) are close to

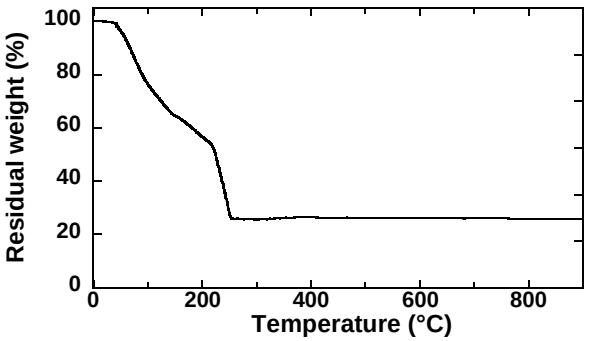

Fig.5 TGA curve of Pre-Zn.

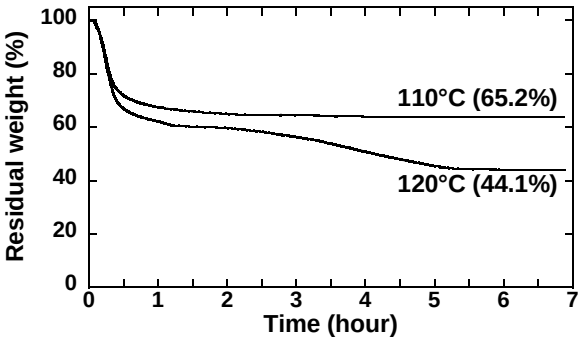

Fig. 6 TGA curves of Pre-Zn kept at 110 and 120 ºC.

the experimental values, the intermediates formed after keeping at 110 and 120 ºC are supposed to be $Zn(NO_3)(OH){\cdot}3H_2O$ and $Zn_3(NO_3)_2(OH)_4$, respectively. The former is soluble in DMAc, whereas the latter is insoluble. Thereby, the former is suitable as a precursor for the *in situ* thermal decomposition method adopted in this study. Hence, $Zn(NO_3)(OH){\cdot}3H_2O$ which is denoted by Pre-Zn(110ºC) was used as the ZnO precursor in Method-2 and Method-3 (see Table 1).

3.3. Optical properties of PI/ZnO hybrid films

3.3.1. Transparencies of the hybrid films

Fig. 7 shows the UV-vis absorption spectra of 6FDA-BAFL/ZnO hybrid films, and the inset depicts the photograph of the films. The yellowish coloration observed for the films prepared by Method-1 and Method-2 should be caused by the nitration reactions occurring in the PAA because nitric acid or NO_3^- ions were generated by thermal decomposition of Pre-Zn (reaction 3). This reaction is essentially the same as xanthoprotein reaction which turns aromatic amino acids or polypeptides to yellow. Since PAA chains possess benzene rings, amide and carboxylic groups, this nitration reaction can proceed effectively. The hybrid films prepared by Method-2 exhibited higher transparency than those prepared by Method-1. The reason is that Pre-Zn(110ºC) contains only a half of nitrate ions per Zn atom than Pre-Zn.

Furthermore, the preparation of hybrid films via

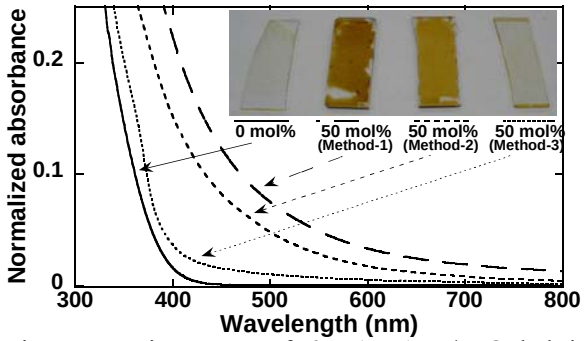

Fig. 7 UV-vis spectra of 6FDA-BAFL/ZnO hybrid films. Inset: photographs of the hybrid films.

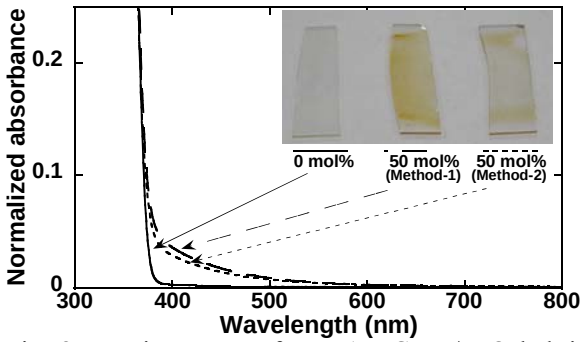

Fig. 8 UV-vis spectra of BPDA-DCHM/ZnO hybrid films. Inset: photographs of the hybrid films.

Method-3 significantly improved the transparency of the films because PI contains no or little amount of amide bonds, which inhibits nitration reactions. Fig. 8 illustrates the UV-vis absorption spectra of BPDA-DCHM/ZnO hybrid films, and the inset depicts photographs of the films. In the same manner as in Fig. 7, the hybrid films prepared by Method-2 exhibited slightly higher transparency than those prepared by Method-1. This also should be due to the lower amount of nitric acid or ions generated from Pre-Zn(110ºC).

3.3.2. IR spectra of hybrid films

The IR spectra of 6FDA-BAFL/ZnO hybrid films are shown in Fig. 9. The peaks observed at 1320 cm^{-1} in the films prepared by Method-1 and Method-2 are assignable to $–NO_2$ groups which cause considerable coloration in the hybrid films. The peak intensity for the Method-1 film is stronger than that for the Method-2 film. In addition, no peak is observed at 1320 cm^{-1} for the Method-3 film, which strongly supports the validity of our assumption that nitration reaction does not occur in PIs due to the lack of amide group. This is consistent with the high transparency of the hybrid films (see Fig. 7).

The IR spectra of BPDA-DCHM/ZnO hybrid films, which is inapplicable to Method-3, are shown in Fig. 10. The intensity of the peak

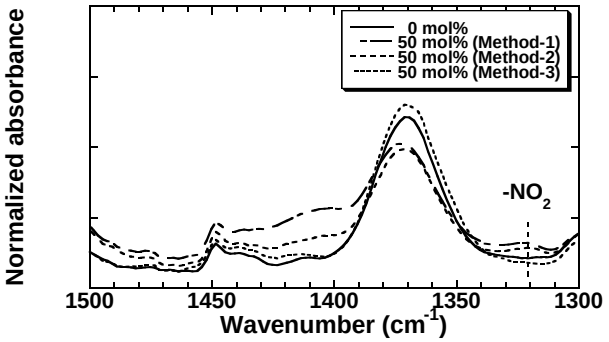

Fig. 9 IR spectra of 6FDA-BAFL/ZnO hybrid films.

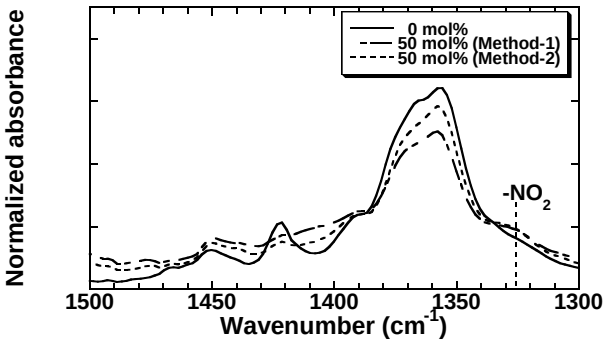

Fig. 10 IR spectra of BPDA-DCHM/ZnO hybrid films.

assignable to nitro groups (1320 cm^{-1}) in the Method-1 film was almost the same as that in the Method-2 film. This also supports the fact that the colorations in the hybrid films is mainly caused by nitration reactions in PAA chains, and the strong yellowish color was generated during thermal decomposition.

3.3.3. Decomposition of Pre-Zn in hybrid films

Fig. 11 illustrates the variable temperature IR spectra of 6FDA-BAFL/ZnO hybrid films prepared via Method-3. Soluble PI solutions containing ZnO precursors were spin-coated onto substrates, followed by drying at 70 ºC for 1 h. The peak observed at 1405 cm^{-1} is assignable to nitrate (NO_3^-) ion. The intensity of this peak has started to decrease from 150 ºC, and the peaks assignable to ZnO at 400~500 cm^{-1} increased above the temperature. The Far-IR spectra of the hybrid films are shown in Fig. 12. The difference spectrum between 0 and 50 mol% of ZnO is consistent with the spectrum of neat ZnO powder (purchased from Fluka). Based on the results in Figs. 11 and 12, it was confirmed that thermal decomposition of Pre-Zn(110ºC) to ZnO was completed at 300 ºC in the PI hybrid films.

3.3.4. TGA analyses of hybrid films

Figs. 13 and 14 show the TGA curves of 6FDA-BAFL/ZnO and BPDA-DCHM/ZnO hybrid films, respectively. The residues after heating at 900 ºC

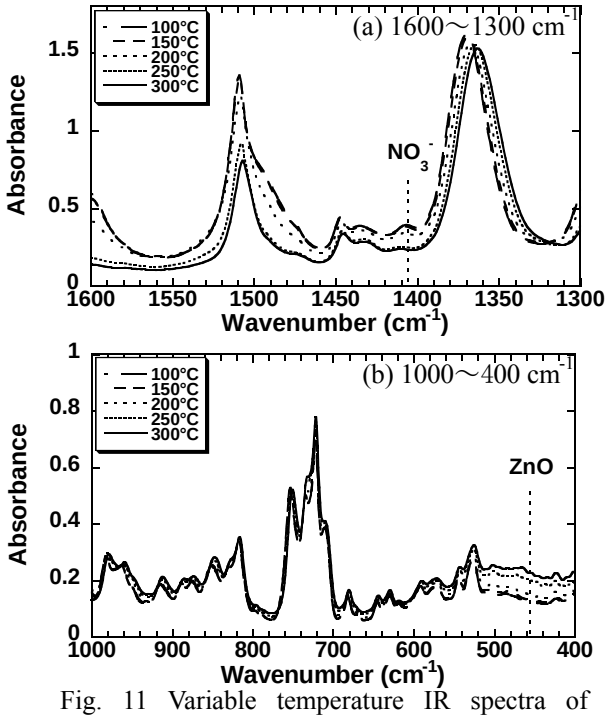

Fig. 11 Variable temperature IR spectra of 6FDA-BAFL/ZnO hybrid films.

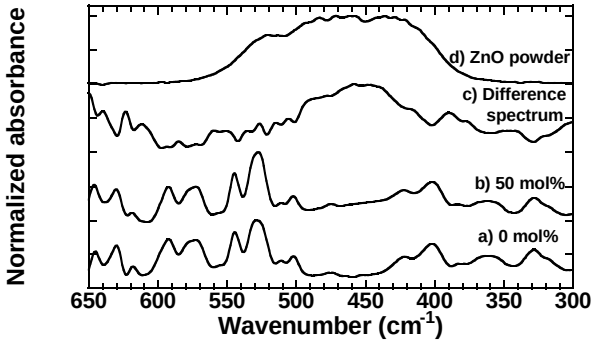

Fig. 12 Far-IR spectra of 6FDA-BAFL/ZnO hybrid films and ZnO (powder).

were consistent with the calculated weights of ZnO. Table 2 lists the 5 % weight-loss temperatures under nitrogen (T_d^5). The T_d^5s of the hybrid films were significantly lower than those of the pristine PIs because ZnO served to catalyze oxidative degradation of the PIs [23]. Nevertheless, the T_d^5s of all the hybrid films were higher than 370 ºC, which indicates that these films exhibited sufficiently high thermal stability compared with the soldering temperature (270 ºC).

3.3.5. Refractive indices of hybrid films

Table 3 lists the refractive indices of PI/ZnO hybrid films measured at the four wavelengths with the estimated values of n_∞ and D based on the equation (2). Fig. 15 shows the wavelength dispersions of refractive indices for (a) 6FDA-BAFL/ZnO and (b) BPDA-DCHM/ZnO hybrid films, respectively. These data clearly

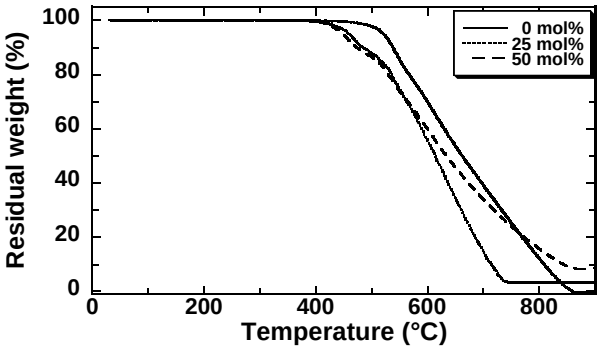

Fig.13 TGA curves of 6FDA-BAFL/ZnO hybrid films (Method-3) under nitrogen.

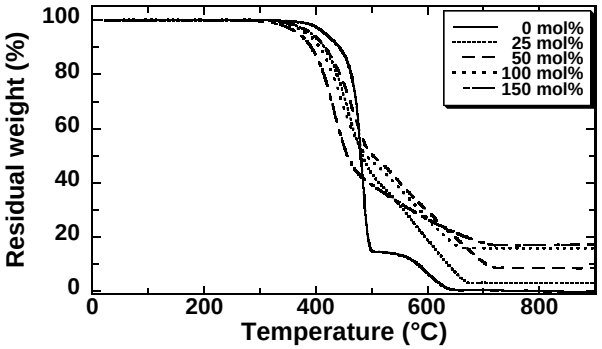

Fig.14 TGA curves of BPDA-DCHM/ZnO hybrid films (Method-2) under nitrogen.

Table 2 5 % weight-loss temperatures of hybrid films.

Polyimide	Zn content (mol%)	T_d^5 (ºC)
6FDA-BAFL	0	521
	25	460
	50	450
BPDA-DCHM	0	419
	25	395
	50	392
	100	384
	150	370

demonstrate that the refractive indices of the hybrid films were increased by the incorporation of ZnO. Hence, the hybridization of PI with ZnO via the *in situ* thermal decomposition method is an effective way to increase the refractive indices of PI films. The changes of n_{av} in the hybrid films at 1324 nm are illustrated in Fig. 16. The n_{av} values were successfully increased by the hybridization with ZnO by up to +0.0037 (0.25%) and +0.0130 (1.10%) for 6FDA-BAFL and BPDA-DCHM, respectively.

On the other hand, the refractive indices of the PI/ZnO hybrid films were theoretically estimated by equation (4) [24],

$$\frac{n_h^2-1}{n_h^2+2} = f_p\frac{n_p^2-1}{n_p^2+2} + f_z\frac{n_z^2-1}{n_z^2+2}, \qquad (4)$$

Table 3 Refractive indices and the coefficient of wavelength dispersions (D) of the hybrid films at 1324 nm.

Polyimide	Zn content (mol%)	n_{633}	n_{845}	n_{1324}	n_{1558}	n_{∞}	D
6FDA-BAFL	0	1.5999	1.5838	1.5739	1.5714	1.5658	13506
	25	1.6042	1.5880	1.5757	1.5733	1.5672	14842
	50	1.6096	1.5934	1.5779	1.5760	1.5692	16367
BPDA-DCHM	0	1.6327	1.6191	1.6088	1.6052	1.6005	12974
	25	1.6367	1.6228	1.6119	1.6087	1.6039	13203
	50	1.6403	1.6262	1.6151	1.6119	1.6070	13416
	100	1.6468	1.6322	1.6207	1.6174	1.6123	13858
	150	1.6530	1.6390	1.6264	1.6231	1.6180	14202

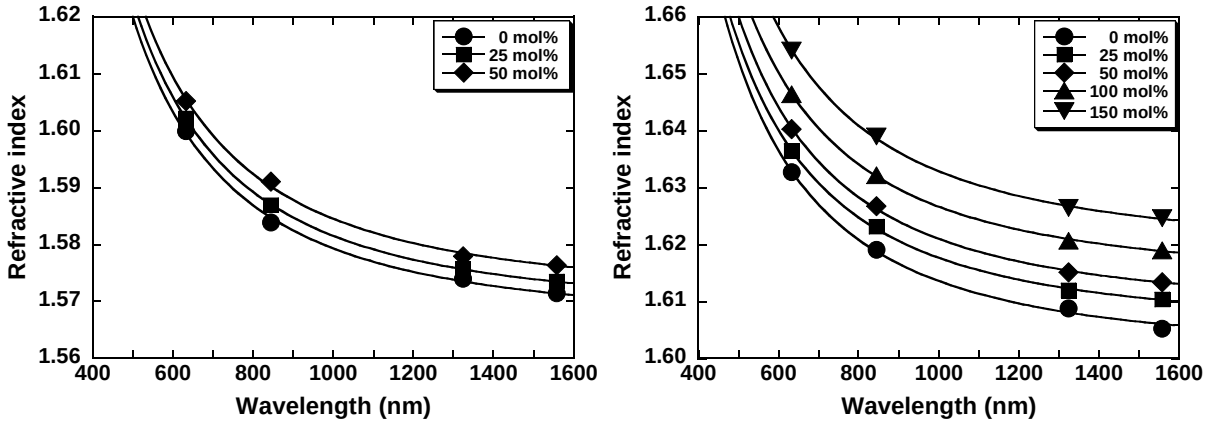

(a) 6FDA-BAFL/ZnO hybrid films (Method-3). (b) BPDA-DCHM/ZnO hyrid films (Method-2).

Fig. 15 Wavelength dispersions of PI/ZnO hybrid films.

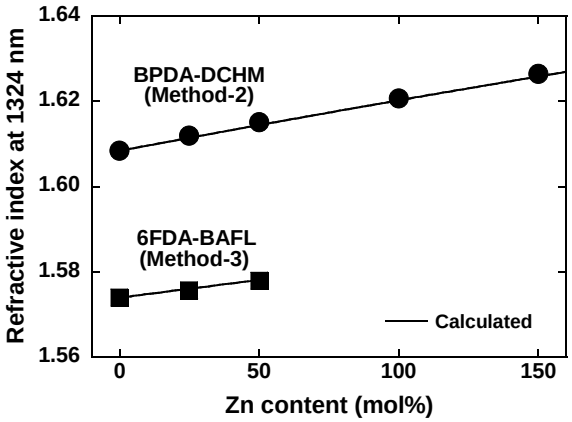

Fig. 16 Refractive index changes of the hybrid films.

where n_h, n_p and n_z are the refractive indices of hybrid film, matrix PI, and ZnO, respectively. f_p and f_z are the volume fractions of PI and ZnO, respectively. Table 4 lists the refractive indices and densities of the matrix PI and crystalline ZnO. Note that the estimated values of n_h agree well with the observed n_{av} values, which supports the complete thermal decomposition from Pre-Zn (110ºC) to ZnO within the PI films (see Figs. 11 and 12). The good agreement between the observed n_{av} and the estimated n_h values suggests the hybridization of PI films with ZnO allows to control the refractive indices of PI films precisely.

Fig. 17 illustrates the relationships between the n_{∞} and D values estimated for the PI/ZnO hybrid films. The slope of the line through 0 and 50 mol% of ZnO for 6FDA-BAFL/ZnO hybrid films prepared by Method-3 (solid line) is larger than that previously reported for fully aromatic PIs (dashed line) [20,21]. This demonstrates that the hybridization of 6FDA-BAFL with ZnO exhibited larger D values than those expected by modifying the chemical structures of PIs. On the other hand, the slope of the line through 0 and 100 mol% of ZnO in the BPDA-DCHM/ZnO hybrid films prepared by Method-2 was smaller than that previously reported for semi-aromatic PIs. This suggests that the hybridization of BPDA-DCHM with ZnO exhibited larger n_{∞} with smaller D values than those expected by modifying the chemical structures. Hence, it was clearly shown that BPDA-DCHM is the best PI matrix for preparing PI/ZnO hybrid films with using $Zn(NO_3)_2 \cdot 6H_2O$ as a precursor. The PI/ZnO hybrid films thus obtained exhibit high refractive indices, high transparencies, and low wavelength dispersions.

Table 4 Refractive indices and densities of the PIs and ZnO.

	n (at 1324 nm)	Density (g/cm^3)
6FDA-BAFL	1.5739	1.45
BPDA-DCHM	1.6088	1.40
ZnO [25]	1.9295	5.60

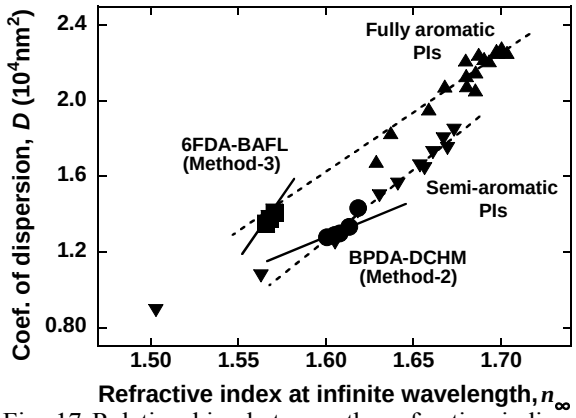

Fig. 17 Relationships between the refractive indices at infinite wavelength (n_∞) and the coefficients of dispersion (D) for the hybrid films.

4. Conclusion

PI/ZnO nano-hybrid films which exhibit high thermal stabilities, high refractive indices, high transparencies, and low wavelength dispersions were successfully prepared via the '*in situ* thermal decomposition method'. The hybrid films prepared from $Zn(NO_3)_2{\cdot}6H_2O$ as a ZnO precursor had coloration caused by nitration reactions of PAAs with NO_3^- ions which were released by the thermal decomposition of the precursor. However, the transparency of the hybrid films were improved by using $Zn(NO_3)(OH){\cdot}3H_2O$ as a ZnO precursor or using a soluble PI solution in place of PAA solution. The hybrid films of 6FDA-BAFL/ZnO and BPDA-DCHM/ZnO exhibited higher refractive indices by up to +0.0037 (+0.25%) and +0.0130 (+1.10%), respectively, as compared with the pristine PIs. The observed n_{av} values agree well with the theoretically estimated values based on the equation involving the refractive indices and the volume fractions of PI and ZnO. This fact suggests that the hybridization of PIs with ZnO enables to control the refractive indices of PI films. In the case of BPDA-DCHM, the effect of hybridization with ZnO on the increase in the refractive index at infinite wavelength (n_∞) relative to the coefficient of wavelength dispersion (D) is more significant than that by modifying the chemical structures of PIs. In addition, the 5 % weight-loss temperatures (T_d^5) of all the hybrid films were higher than 370 ºC. In consequence, it was confirmed that the hybridization of semi-aromatic PIs with ZnO using $Zn(NO_3)_2{\cdot}6H_2O$ as a precursor is a facile and promising way to prepare thin PI films exhibiting high refractive indices, high transparencies, and low wavelength dispersions without deteriorating their high thermal stability and good mechanical properties.

References

1. J. -G. Liu and M. Ueda, *J. Mater. Chem.*, **19** (2009) 8907.
2. S. Ando, *J. Photopolym. Sci. Technol.*, **17** (2004) 219
3. A. Terraza, J. -G. Liu, Y. Nakamura, Y. Shibasaki, S. Ando and M. Ueda, *J. Polym. Sci. Part A: Polym., Chem.*, **46** (2008) 1510.
4. Y. Watanabe, Y. Sakai, Y. Shibasaki, S. Ando and M. Ueda, *Macromolecules*, **35** (2002) 2277.
5. J. -G. Liu, Y. Nakamura, T. Ogura, Y. Shibasaki, S. Ando and M. Ueda, *Chem. Mater.*, **20** (2008) 273.
6. S. Lee, H. -J. Shin, S. -M. Yoon, D. K. Yi, J. -Y. Choi and U. Paik, *J. Mater. Chem.*, **18** (2008) 1751.
7. M. M. Demir, K. Koynov, Ü. Akbey, C. Bubeck, I. Park, I. Lieberwirth and G. Wegner, *Macromolecules*, **40** (2007) 1089.
8. D. Yorifuji, A. Matsumura, T. Aoki, Y. Tashiro, S. Kuroki and S. Ando, *J. Photopolym. Sci. Technol.*, **22** (2009) 447.
9. T. Matsui and M. Kondo, *Appl. Phys. Lett.*, **88** (2006) 183508.
10. S. Ito, Y. Makari, T. Kitamura, Y. Wada and S. Yanagida, *J. Mater. Chem.*, **14** (2004) 385.
11. X. W. Sun, B. Ling, J. L. Zhao, S. T. Tan, Y. Yang, Y. Q. Shen, Z. L. Dong and X. C. Li, *Appl. Phys. Lett.*, **95** (2009) 133124.
12. C. -H. Lai, W. -F. Lee, I. -C. Wu, C. -C. Kang, D. -Y. Chen L. -J. Chen and P. -T. Chou, *J. Mater. Chem.*, **19** (2009) 7284.
13. A. Somwangthanaroj, K. Suwanchatchai, S. Ando and W. Tanthapanichakoon, *Mater. Chem. Phys.*, **114** (2009) 751.
14. J. Wu, S. Yang, S. Gao, A. Hu, J. Liu and L. Fan, *Euro. Polym. J.*, **41** (2005) 73.
15. S. -L. Huanga, W. -K. Chin and W. -P. Yang, *Polymer*, **46** (2005) 1865.
16. N. Nakayama and T. Hayashi, *J. Appl. Polym. Sci.*, **105** (2007) 3662.
17. Y. Li, S. -Y. Fu, Y. -Q. Li, Q. -Y. Pan, G. Xu and C. -Y. Yue, *Comp. Sci. Technol.*, **67** (2007) 2408.
18. T. Sawada and S. Ando, *Chem. Mater.*, **10** (1998) 3368.
19. Y. Oishi, K. Ogasawara, H. Hirahara and K. Mori, *J. Photopolym. Sci. Technol.*, **14** (2001) 37.
20. S. Ando, Y. Watanabe and T. Matsuura, *Jpn. J. Appl. Phys.*, **41** (2002) 5254.
21. S. Ando, *Proc. SPIE*, **7213** (2009) 72130B.
22. A. J. Kozak, K. W. Ciurowa and A. Kozak, *J. Therm. Anal. Cal.*, **74** (2003) 497.
23. R. K. Boggess and L. T. Taylor, *J. Polym. Sci., Polym. Chem. Ed.* **25** (1987) 685.
24. Q. Chen, M. R. Lin, J. E. Lee, Q. M. Zhang and S. Yin, *Appl. Phys. Lett.*, **89** (2006) 141121.
25. D. R. Lide "*Handbook of Chemistry and Physics 86th Edition*", Taylor & Francis (2005).